THEMIS multi-spacecraft observations of magnetosheath plasma penetration deep into the dayside low-latitude magnetosphere for northward and strong B_y IMF

M. Øieroset[(1)], T. D. Phan[(1)], V. Angelopoulos[(2)], J. P. Eastwood[(1)], J. McFadden[(1)], D. Larson[(1)], C. W. Carlson[(1)], K.-H. Glassmeier[(3)], M. Fujimoto[(4)], J. Raeder[(5)]

1. Space Sciences Laboratory, University of California at Berkeley, CA USA
2. IGPP/ESS, UCLA, Los Angeles, CA USA
3. TUBS, Braunschweig, D-38106, Germany
4. JAXA
5. UNH

Index terms:

Abstract

On 2007-06-03 the five THEMIS spacecraft consecutively traversed the dayside (13.5 MLT) magnetopause during northward IMF with strong B_y. While one spacecraft monitored the magnetosheath, the other four encountered a persistent and extended region of nearly-stagnant magnetosheath plasma attached to the magnetopause on closed field lines. This region was much denser than, but otherwise similar to, the nightside cold-dense plasma sheet. At one point this region was bordered by two spacecraft, allowing the direct determination of its thickness of 0.9 R_E. There was no evidence for Kelvin-Helmholtz waves nor diffusion at the local magnetopause. The characteristics of the particle distributions suggest that substantial solar wind entry across the dayside magnetopause occurred as a result of reconnection in both cusps involving the same field lines, resulting in trapping of plasma on the nose of the magnetosphere, sunward of 13.5 MLT, even when the IMF clock angle was as large as 60^o.

1. Introduction

It is commonly believed that the dominant process by which the solar wind enters the Earth's magnetosphere is via dayside and nightside reconnection during southward IMF [Dungey, 1961]. The magnetosphere was thought to be more closed to the solar wind during northward IMF. In such a scenario, one would expect that density of solar wind-sourced material in the plasma sheet would decrease during northward IMF.

Surprisingly, however, the opposite behavior is observed. The plasma density in the near-Earth nightside plasma sheet during northward IMF is ~1 cm^{-3}, three times that observed during southward IMF. The plasma temperature is lower during northward IMF [e.g., Fujimoto et al., 1996; Terasawa et al., 1997; Øieroset et al., 2002]. This cold and dense plasma sheet (CDPS) has been detected deep inside the magnetosphere and often consists of a mixture of magnetosheath and magnetospheric plasma [e.g., Fujimoto et al., 1996; Fuselier er al., 1999; Phan et al., 2000; Nishino et al., 200?; Hasegawa et al., 200?]. During prolonged periods of strongly northward IMF the CDPS can fill the entire near-Earth plasma sheet [Øieroset et al., 2005]. The CDPS could have significant impact on inner-magnetospheric dynamics during strong convection times as the earthward injection of the denser plasma contributes to the development of an enhanced ring current [e.g., Thomsen et al., 2003]. Determining the processes by which the CDPS is formed is thus one of the key challenges in magnetospheric physics.

Several transfer processes have been suggested including (1) slow diffusion of solar wind plasma across the flank low-latitude boundary layer (LLBL) [Terasawa et al., 1997], (2) capture of solar wind plasma by non-linear Kelvin-Helmholtz instabilities on the flank magnetopause [Fujimoto and Terasawa, 1994; Hasegawa et al. , 2004], and (3) capture of magnetosheath plasma by poleward-of-cusp reconnection in both hemispheres [Song and Russell, 1992; Raeder et al., 1995; Li et al., 2005]. However, the relative importance of these processes and the locations where they dominate are still unknown, largely because of the lack of simultaneous multi-point observations at the key entry sites.

In this letter we use the uniqueness of the THEMIS coast phase orbits to investigate the transfer of solar wind plasma into the dayside magnetosphere during a prolonged interval of northward IMF with strong B_y. Using multi-spacecraft THEMIS observations we report the first direct measurement of the thickness of the dayside CDPS and investigate the temporal evolution of particle distributions in this layer.

This letter is organized as follows. First we briefly describe the orbits and instrumentation. We then present single spacecraft observations of the dayside cold-dense plasma sheet to illustrate in detail its properties, followed by the descriptions of the similarity and differences in the CDPS properties observed by the various spacecraft. Lastly, we discuss the implications of the present observations for the solar wind entry mechanisms.

2. Orbits and Instrumentation

On June 3, 2007, between 15:22:00 and 17:11:00 UT, the five THEMIS spacecraft traversed the dayside (13.5 MLT) magnetopause in a string of pearls configuration in an outbound pass with the spacecraft in the following order: B, D, C, E, A (Figure 1). The THEMIS mission was in its coast phase with all five spacecraft in the same 14.7 R_E apogee orbit. The separations between spacecraft were nearly radial near the magnetopause, with the leading and trailing spacecraft separated by ~2 R_E and the middle three spacecraft separated by ~4000 km. In this paper we use 3-s resolution data from the fluxgate magnetometer [Auster et al., 2008] and the ion and electron instruments [McFadden et al., 2008]. We use data from ACE to monitor the solar wind conditions. The propagation time from ACE to the magnetopause was determined by comparing the ACE and THEMIS-B magnetic field observations when THEMIS-B was located in the magnetosheath.

3. THEMIS-A single spacecraft observations

TH-A was the trailing spacecraft in the pearls-on-a-string configuration. Figure 2 shows the outbound pass by the TH-A spacecraft through the regions surrounding the 13.5 MLT magnetopause. In the interval shown, the spacecraft started out in the magnetosphere proper where there were only single energetic ion (Fig. 2c) and electron (Fig. 2d) populations, and ended up in the magnetosheath where the flow speed was > 100 km/s. Between the hot (T_i~ 5 keV) and tenuous (N_i~ 0.2 cm^{-3}) magnetosphere and the magnetosheath, TH-A observed, for more than half an hour (from 16:31:10-17:05:10 UT marked by the horizontal dark blue bar in Fig. 2c), a nearly stagnant (Fig. 2g) and mixed population of both magnetospheric and heated magnetosheath ions with density and temperature intermediate between magnetospheric and magnetosheath values. There was a gradual density gradient toward the magnetopause, with the ion density increasing from ~ 1 cm^{-3} at the inner edge of the mixed ion region (at 16:31:10 UT) to 3.8 cm^{-3} (at 17:05 UT) near the magnetopause, the average density being ~ 3.3 cm^{-3}. The magnetic field in this region was extremely smooth. The plasma and field properties of this region are similar to those of the CDPS commonly observed further downtail and in the nightside plasma sheet during northward IMF, except that the density in this dayside CDPS is 3 times higher than in the typical nightside CDPS. Figure 2h shows the velocity component tangential to the magnetopause, v_M, with negative v_M being tailward. The tangential flow speed in the CDPS was low (< 40 km/s) and its direction was highly variable showing no systematic tailward or earthward flow. The nearly-stagnant plasma and smooth magnetic field in this CDPS stand in contrast to the flowing and more turbulent Low-Latitude Boundary Layer (LLBL).

The CDPS interval was interrupted by a ~1 minute interval near 17:02 UT with N_i > 10 cm^{-3} and T_i ~ 100 eV, indicating a brief excursion into the magnetosheath. Between the end of the CDPS at 17:05:00 UT and the magnetopause crossing at 17:11:10 UT, TH-A re-encountered the single-population hot magnetosphere. Although the CDPS appears to be detached from the magnetopause, this may not be a spatial effect as will be discussed later.

In addition to the mixed ions, Fig. 2d shows the presence of mixed magnetospheric and heated magnetosheath electrons during the earlier part of the CDPS (marked by the light blue bar in Fig. 2d). Figure 3 shows an electron pitch-angle distribution sampled at 16:39:32 UT inside the mixed electron region. The field-aligned and anti-field-aligned electron fluxes of both (high-energy) magnetospheric and (low-energy) magnetosheath origin are well balanced. In the outer CDPS where there was only a single heated magnetosheath electron population, the field-aligned and anti-field-aligned electron fluxes were also well balanced. These electron behaviors indicate that the entire CDPS was on closed field lines. Note that the energetic magnetospheric electrons inside the mixed-ion CDPS have rarely been reported in previous CDPS events. In the present event, the thickness of this mixed electron layer appears to evolve with time as will be discussed in the next section.

The CDPS observed by TH-A occurred during a period of relatively steady northward and dawnward IMF, except for a brief 3-min interval (17:00-17:03 UT) when the IMF had a southward component.

4. Solar wind and five-spacecraft THEMIS observations

4.1. Solar wind and IMF conditions

Figures 4a-c display the time-shifted solar wind dynamic pressure, the IMF, and the IMF theta angle (θ_{IMF}= $\tan^{-1}[B_{z,GSM}/|B_{y,GSM}|]$), respectively, observed by ACE during the interval of interest. At the beginning of the interval the IMF was southward-directed (θ_{IMF} ~ -90^o). At 15:25 UT, the IMF abruptly turned to dominantly duskward (θ_{IMF} ~0^o). Over the next 35 minutes, the IMF became increasingly more northward, with θ_{IMF} varying linearly from 0^o to ~ 70^o during that interval. This interval was followed by one hour (16:00-17:00 UT) of relatively steady northward and dawnward IMF, with θ_{IMF} varying between 30^o-70^o. At 17:00 UT the IMF turned southward for 3 minutes followed by a brief interval of northward IMF before becoming dominantly southward after 17:07 UT. The varying but well-defined IMF orientation during the two hours of interest provided important information on the IMF condition for the occurrence of the CDPS. Finally, the solar wind dynamic pressure varied between 1.5 nPa and 3.5 nPa during the two-hour interval.

4.2. THEMIS five-spacecraft observations

Figure 4 d-r show observations from all five THEMIS spacecraft as they traversed one after another the regions surrounding the magnetopause (MP). The multi-spacecraft observations allow the solar wind conditions under which the CDPS was detected to be investigated as well as the temporal versus spatial evolution of the region to be explored.

TH-B (Fig. 4d, i, and n) was the leading spacecraft and encountered the magnetopause at 15:22:00 UT, while the IMF was southward-directed. The duration of the MP/LLBL crossing was only ~1 minute, in contrast to the duration of the TH-A crossing of the CDPS (> 30 minutes). The TH-B crossing occurred during a period of stable solar wind ram pressure (Fig. 4a) and did not coincide with the sudden increase of the ram pressure that accompanied the northward turning of the IMF 3 minutes later. The 1-min duration of the crossing must therefore imply a thin MP/LLBL during southward IMF. After the crossing, TH-B served as the magnetosheath monitor and was used to determine the exact time lag for the ACE data.

Before the IMF turned northward at 15:25:00 UT, the remaining four spacecraft (D, C, E, and A) were located inside the hot magnetosphere. Starting at 15:51:00 UT all four spacecraft consecutively encountered the CDPS marked with the dark blue bars in Figure 3. In fact, TH-D started to intermittently encounter the CDPS when $\theta_{IMF} \sim 11^o$, at 15:29:22 UT, prior to detecting the CDPS in a more continuous fashion. The magnetosheath-like plasma encountered by TH-D, C, and E had similar properties as the CDPS observed by TH-A (section 3), i.e., it was stagnant, with stable magnetic field, heated magnetosheath ions and electrons, and field-aligned and anti-field aligned electron fluxes that were well balanced at all energies (not shown), indicating that this region was on closed field lines. TH-E observed the highest average CDPS density of 6.7 cm^{-3}, while the average densities in the TH-D, C, and E CDPS were ??, ??. and ??, respectively, all of which are much higher than the density in the nightside CDPS. Combining all four spacecraft, the CDPS was observed continuously from 15:51:00 UT (TH-D) to 17:05:10 UT (TH-A). Thus the CDPS was a persistent spatial region over 74 minutes, during which time θ_{IMF} varied between 30^o and 70^o.

Although TH-D, TH-C, and TH-E detected a CDPS with similar properties to the one encountered later by TH-A there were some notable differences. Unlike TH-A, which observed a mixture of magnetospheric and heated magnetosheath ions, the plasma observed by TH-D was for the most part not mixed, with the magnetospheric component being absent or weak. The magnetospheric ions were clearly present in more than half of the TH-C CDPS samples, and they were present throughout the TH-E CDPS observations. Thus the magnetosheath-sourced CDPS ions appeared to become more mixed with increasingly higher fluxes of hot magnetospheric ions as time progressed.

The electrons display a similar feature. At the beginning of the CDPS interval TH-D, C, and E observed single population electrons with peak energies of 100 eV, i.e., heated magnetosheath electrons, while hot (5-10 keV) magnetospheric electrons were absent. Towards the end of the CDPS interval, however, TH-A observed both cold and hot electrons inside the CDPS 75% of the time (marked by the light blue bar in Figure 2d).

Unlike TH-A, TH-D, C, and E all observed the CDPS to be attached to the magnetopause. The magnetopause crossings by these three spacecraft occurred during northward IMF and were all single crossings, indicating that there were no surface waves present at 13.5 MLT. TH-A exited the CDPS 5 minutes before encountering the magnetopause, during which time it observed an interval of hot magnetospheric plasma. The difference between the TH-A observations and the other probes may be related to the southward turning of the IMF five minutes earlier at 17:00:00 UT, as observed by TH-B and ACE.

The large variation in the solar wind dynamic pressure meant that we could not reliably determine the CDPS thickness using single spacecraft measurements. The variation in the dynamic pressure also meant that the evolution of the CDPS thickness could not be determined from the relative CDPS duration at the various spacecraft. However, at around 16:30 UT THEMIS-C crossed the magnetopause (outer edge of the CDPS) while TH-A entered the CDPS. Thus the two spacecraft bordered the CDPS, allowing its thickness to be determined directly. The CDPS thickness was found to be 1.1 R_E along the spacecraft track, or ~0.9 R_E normal to the magnetopause.

5. Discussion

The event presented here shows the persistent presence of a thick (0.9 R_E) dayside CDPS of magnetosheath-like but nearly-stagnant plasma immediately earthward of the magnetopause at 13.5 MLT. This CDPS was on smooth and closed field lines and was observed continuously when the IMF theta angle was between 30^o and 70^o (or IMF clock angle between 60^o and 20^o). The multi-spacecraft observations revealed the evolution of the ion and electron distributions in the CDPS, showing the increasing presence of the hot magnetospheric ions and electrons in the CDPS with time. We now discuss these observations in relation to the candidate solar wind entry processes: diffusive entry, Kelvin-Helmholtz instabilities, and dual-lobe reconnection.

Even though there was a slight density gradient from the inner edge of the CDPS to the MP, which could be consistent with diffusive entry, the CDPS was observed on extremely smooth magnetic field with no notable wave activity. Thus it is unlikely that diffusive entry across the local magnetopause is important for the formation of the observed CDPS at 13.5 MLT.

There was also no evidence for Kelvin Helmholtz (K-H) activity at the local magnetopause since the magnetopause appears to be a stable boundary with no boundary waves. The absence of K-H waves at 13.5 MLT under normal solar wind condition is not unexpected.

It is also unlikely that the present CDPS at 13.5 MLT is the result of plasma entry via diffusive entry or K-H further downtail and subsequent sunward convection. Such a scenario is not expected to result in a thin (0.9 R_E) CDPS attached to the magnetopause on the dayside. Furthermore, there was no systematic sunward flow observed in the CDPS.

The likely source of the present dayside closed field CDPS is the capture of magnetosheath plasma by poleward-of-cusp reconnection in both hemispheres [Song and Russell, 1992; Raeder et al., 1995]. The key evidence for dual-lobe reconnection in this event is the presence of counterstreaming and heated magnetosheath electrons on CDPS field lines. Such electrons have previously been observed in the magnetosheath boundary layer just outside the magnetopause and interpreted as evidence for the capturing and closing of the magnetosheath field lines by dual-lobe reconnection during northward IMF

[Onsager et al., 200?, Lavraud et al., 2006, McFadden et al., this volume]. The fact that the CDPS is seen at 13.5 MLT for IMF theta angle of 30-70 degrees implies not only that reconnection occurred on the same field lines in both cusps, but that this results in the addition of magnetic flux to the subsolar magnetosphere, even when the IMF has a strong B_y component. More importantly, this scenario led to substantial and persistent entry of the solar wind across the dayside magnetopause as evidenced by the uninterrupted (for 74 minutes) encounter of a rather thick (0.9 Re) CDPS that was attached to the magnetopause until the IMF turned southward.

Although the dual-lobe reconnection scenario enables the capture of magnetosheath plasma, it does not immediately explain the simultaneous presence of 10 keV magnetospheric ions and 5-10 keV electrons. The fact that these energetic particles in the CDPS have the same energy as (and their flux levels are similar to or lower than) those observed in the adjacent (hot) magnetosphere suggest a local source which penetrates via magnetic gradient and curvature drifts. The fact that the intensity and the depth of penetration of the energetic ions and electrons into the CDPS increase with time seems consistent with this scenario.

Ultimately what one wishes to know observationally is whether the dayside CDPS could be the source of the much thicker nightside CDPS as has been suggested by global simulations [Raeder et al., 1995; Li et al., 2005]. The fact that the density in this dayside CDPS is 3-6 times higher than the typical value observed in the nightside CDPS is consistent with the expected increase of the magnetic flux tube volume associated with the transport of CDPS flux tubes from the dayside to the nightside. However, the observed tangential flow velocity did not show a systematic tailward flow which would be expected under this scenario. Instead THEMIS observed alternating sunward and tailward slow (10-40 km/s) flows in the CDPS. This could imply that the transport is slow and not laminar. The slow transport may be consistent with previous studies showing that the CDPS is observed in the magnetotail only several hours after a northward IMF turning [Terasawa et al., 1997; Oieroset et al., 2002; 2005].

To fully solve this problem, the present THEMIS observations need to be put in a more global context. Comparisons with Geotail observations on the dawn flank and with global simulations could shed lights on the question regarding plasma transport as well as the relative importance of the different candidate solar wind entry processes at different magnetopause locations. It is possible that several processes may be active at the same time but at different magnetopause locations [e.g., Taylor et al., 2007].

Acknowledgments

This work was supported by NASA grant NAS5-02099. The work of KHG was financially supported by the German Ministerium für Wirtschaft und Technologie and the German Zentrum für Luft- und Raumfahrt under grant 50QP0402.

References

Figure 1. THEMIS orbit and spacecraft locations on June 3, 2007 in the vicinity of the 13.5 MLT magnetopause.

Figure 2. (a) The time-shifted IMF measured by ACE. (b-h) THEMIS-A measurements of the magnetic field, ion and electron energy spectrograms, ion density, temperature and velocity, and the M component of the velocity tangential to the magnetopause and perpendicular to the magnetic field, respectively. The LMN boundary coordinate system is defined such that N is along the model magnetopause normal and the L-M plane is tangential to the magnetopause with M approximately due west. The horizontal dark blue bar in (c) marks the CDPS region. The light blue bar in (d) denotes the region of mixed magnetosheath and magnetospheric electrons.

Figure 3. Electron pitch-angle distribution measured by TH-A in the mixed electron region. The field-aligned and anti-field-aligned electrons are well balanced indicative of closed field topology.

Figure 4. Solar wind conditions and five spacecraft observations of the dayside cold-dense plasma sheet. (a-c) Solar wind ram pressure, magnetic field, and magnetic field theta angle ($\theta_{IMF}= \tan^{-1}[B_{z,GSM}/|B_{y,GSM}|]$). (d-h) magnetic field components, (i-m) ion spectrograms, and (n-r) electron spectrograms from THEMIS B, D, C, E, A respectively. The horizontal dark blue bars mark the CDPS intervals. The magnetopause marked by a vertical black line, corresponds to the open/closed field boundary deduced from the electron pitch angle distributions.

Deleted: ¶
¶

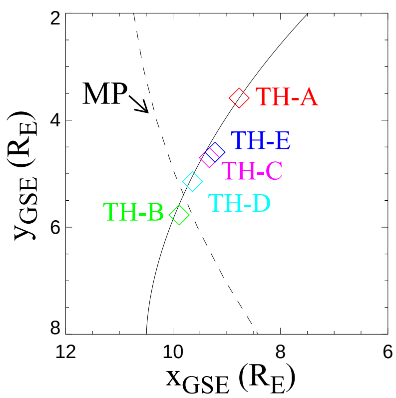

Figure 1

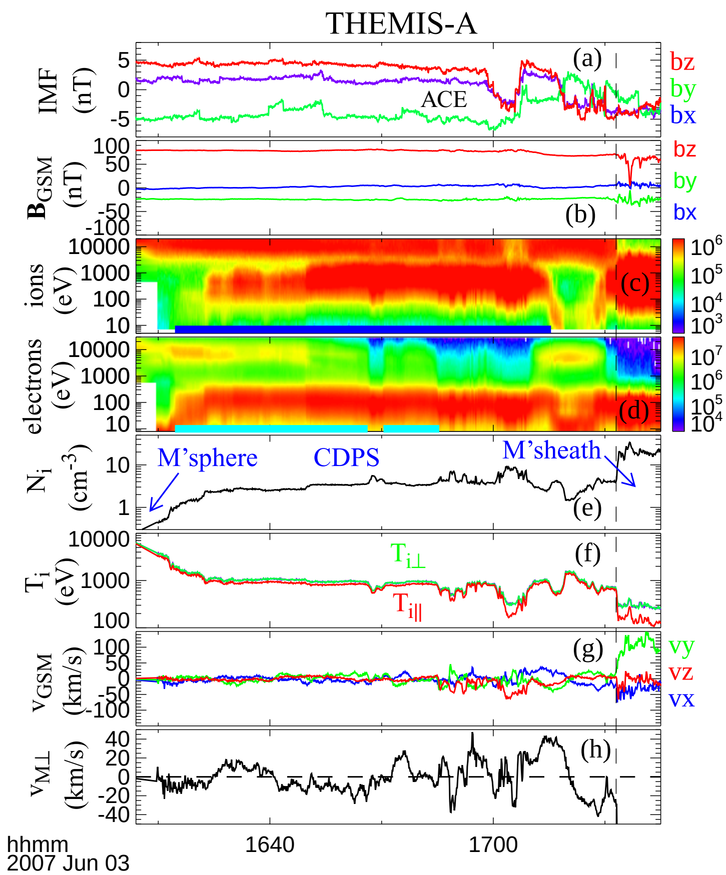

THEMIS-A
IMF (nT)
ACE
(a)
bz
by
bx
B_GSM (nT)
(b)
ions (eV)
(c)
electrons (eV)
(d)
N_i (cm^-3)
M'sphere
CDPS
M'sheath
(e)
T_i (eV)
T_i⊥
T_i||
(f)
v_GSM (km/s)
(g)
vy
vz
vx
v_M⊥ (km/s)
(h)
hhmm
2007 Jun 03
1640
1700

Figure 2

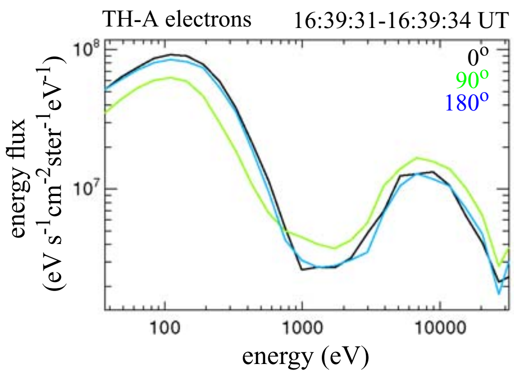
TH-A electrons
16:39:31-16:39:34 UT
0°
90°
180°
energy flux
(eV s^{-1}cm^{-2}ster^{-1}eV^{-1})
energy (eV)
10⁸
10⁷
100
1000
10000

Figure 3

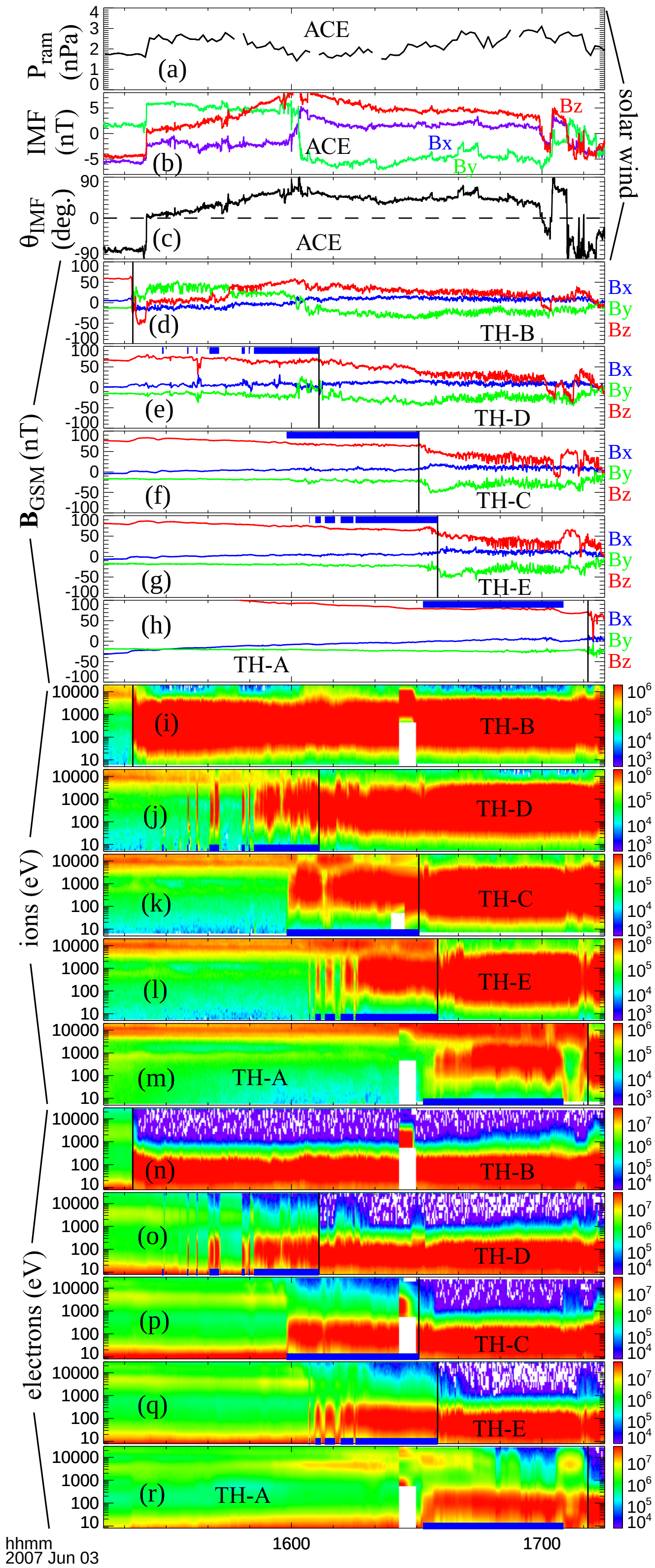

P_ram (nPa)
ACE
(a)
IMF (nT)
Bz
Bx
By
(b)
θ_IMF (deg.)
(c)
solar wind
B_GSM (nT)
(d) TH-B
(e) TH-D
(f) TH-C
(g) TH-E
(h) TH-A
Bx
By
Bz
ions (eV)
(i) TH-B
(j) TH-D
(k) TH-C
(l) TH-E
(m) TH-A
electrons (eV)
(n) TH-B
(o) TH-D
(p) TH-C
(q) TH-E
(r) TH-A
hhmm
2007 Jun 03
1600
1700

Figure 4

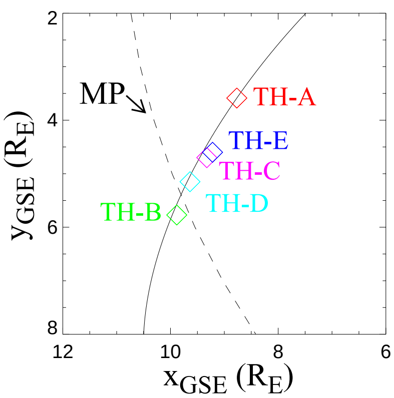

Figure 1

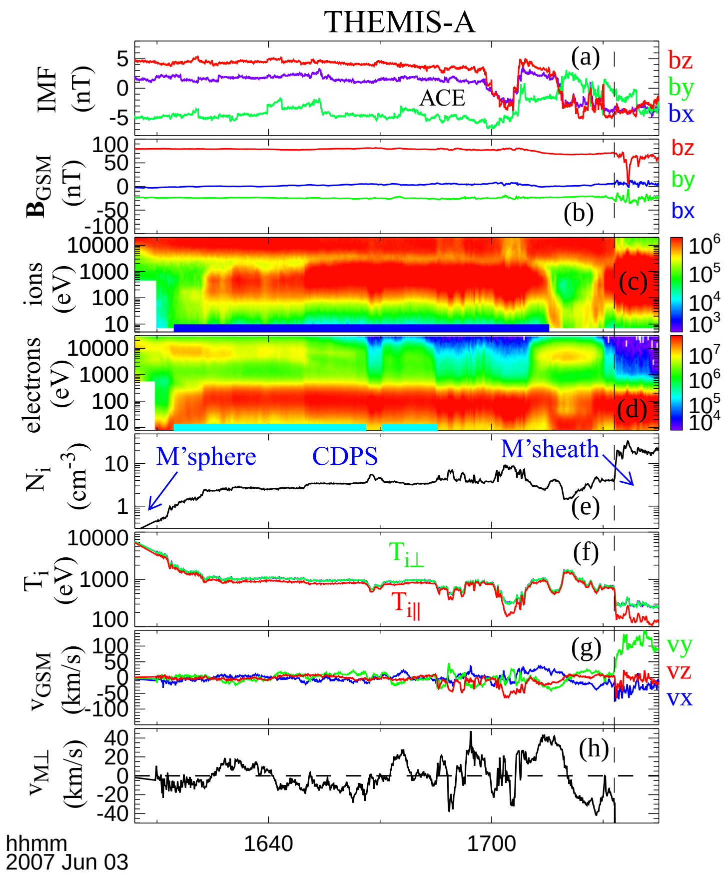
THEMIS-A
IMF (nT)
(a)
ACE
bz
by
bx
B_GSM (nT)
(b)
ions (eV)
(c)
electrons (eV)
(d)
N_i (cm^-3)
M'sphere
CDPS
M'sheath
(e)
T_i (eV)
T_i⊥
T_i||
(f)
v_GSM (km/s)
(g)
vy
vz
vx
v_M⊥ (km/s)
(h)
hhmm
2007 Jun 03
1640
1700

Figure 2

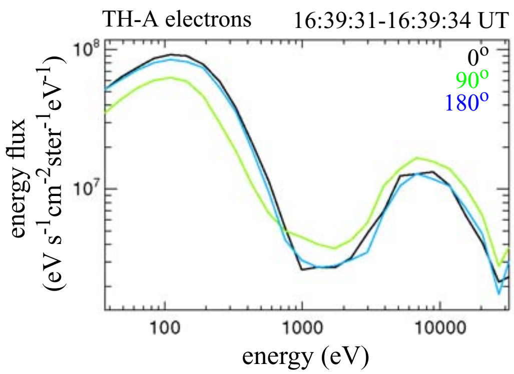
TH-A electrons
16:39:31-16:39:34 UT
0°
90°
180°
energy flux
(eV s^{-1}cm^{-2}ster^{-1}eV^{-1})
10^8
10^7
100
1000
10000
energy (eV)

Figure 3

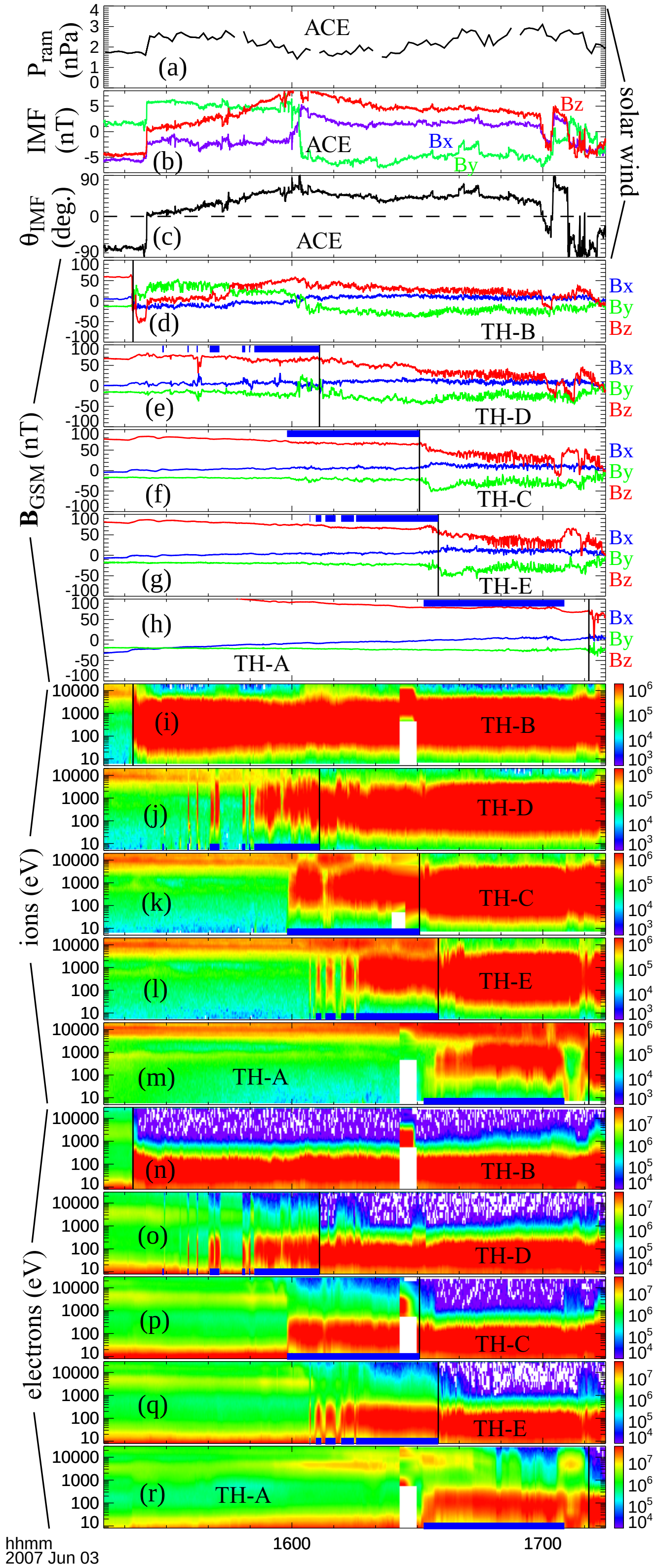

ACE
(a)
(b)
(c)
Bz
Bx
By
solar wind
(d) TH-B
(e) TH-D
(f) TH-C
(g) TH-E
(h) TH-A
(i) TH-B
(j) TH-D
(k) TH-C
(l) TH-E
(m) TH-A
(n) TH-B
(o) TH-D
(p) TH-C
(q) TH-E
(r) TH-A
ions (eV)
electrons (eV)
hhmm
2007 Jun 03
1600
1700

Figure 4